SPECIAL REPORT 91-20

(2)

CRREL

Buckling of Unidirectional Graphite/Epoxy Composite Plates at Low Temperatures

Piyush K. Dutta, David Hui, and Yvonne M. Traynham

November 1991

For conversion of SI metric units to U.S./British customary units of measurement consult ASTM Standard E380, Metric Practice Guide, *published by the American Society for Testing and Materials, 1916 Race St., Philadelphia, Pa. 19103.*

This report is printed on paper that contains a minimum of 50% recycled material.

Special Report 91-20

U.S. Army Corps
of Engineers
Cold Regions Research &
Engineering Laboratory

Buckling of Unidirectional Graphite/Epoxy Composite Plates at Low Temperatures

Piyush K. Dutta, David Hui, and Yvonne M. Traynham

November 1991

Prepared for
OFFICE OF THE CHIEF OF ENGINEERS

PREFACE

This report was prepared by Dr. Piyush K. Dutta, Materials Research Engineer, of the Applied Research Branch, Experimental Engineering Division, U.S. Army Cold Regions Research and Engineering Laboratory, Dr. David Hui, Associate Professor of Mechanical Engineering, University of New Orleans, and Yvonne Traynham, graduate student, University of New Orleans. The work was carried out in the Materials Research Laboratory of CRREL. Funding for this work was provided by DA Project 4A762784AT42, *Design, Construction and Operations Technology for Cold Regions,* Task SS, Work Unit 019, *Behavior of Materials at Low Temperatures.*

The authors express their appreciation to Dr. Arnold H. Mayer, Assistant for Research and Technology, Air Force Wright Aeronautical Laboratory, Flight Dynamics Laboratory, Dayton, Ohio, and Dr. Devinder S. Sodhi of CRREL for reviewing the report and providing very helpful and valuable suggestions. The authors also thank John Kalafut of CRREL for providing much needed support and participation in the experimental measurement program. Special thanks are given to Frederick Gernhard of the Machine Shop at CRREL for building the test fixtures and support mounts.

Buckling of Unidirectional Graphite/Epoxy Composite Plates at Low Temperatures

PIYUSH K. DUTTA, DAVID HUI, AND YVONNE M. TRAYNHAM

INTRODUCTION

Buckling and postbuckling behavior of composite material plates has been thoroughly investigated because of their many aerospace, automotive, marine and sporting goods applications (Singer 1985, Leissa 1985, Chen and Chen 1987, Biswas 1976, Chen et al. 1985, Flaggs and Vinson 1978, Jones 1975). Surprisingly, such behavior under cold environments has received only scant attention. Even in the simple case of unidirectionally graphite-epoxy material plates, no buckling studies have been reported in the literature.

The objective of this investigation is to study the effect of low temperatures on the unidirectional graphite epoxy laminate plates in the buckling mode when they are constrained and loaded in the direction of the fibers. The current work is particularly interesting since such graphite/epoxy plates, due to their negative thermal expansion coefficients, expand in the fiber direction under cooling, whereas in most conventional materials, lowering the temperature will cause contraction. Under in-plane constraint, such graphite-epoxy plates may develop out-of-plane bending under cooling even without any mechanical load. Thus, upon bending, the in-plane load carrying capacity of the plate may be significantly reduced. The same observation can be made on thermal heating of other conventional materials having positive thermal expansion coefficients. Normally, a plate made of conventional material becomes stiffer under thermal cooling and the critical buckling load is expected to be higher. But, in the case of unidirectional graphite-epoxy plates under cooling, there are two opposing effects: the structure becomes stiffer (advantage) and, in the presence of in-plane constraint, the structure will bend due to expansion (disadvantage). Thus, it is of interest to determine which effect will dominate in the buckling problems. The analysis presented here is novel in that the plate bending due to thermal cooling is treated as an initial geometric imperfection in the buckling and postbuckling investigation. The basic findings of the unidirectionally laminated plate will enhance the understanding of the buckling behavior of composite plates under thermal environments.

In the current study, a number of unidirectional graphite-epoxy laminated plates were tested at room and low temperature under uniaxial compressive load. To determine the bending strains, the plates were instrumented with strain gauges mounted on both sides of their surfaces at the center. The load was applied in a servohydraulic testing machine, and strains were recorded using a data acquisition system.

BUCKLING OF PLATES UNDER THERMO-MECHANICAL LOADS

The bending of the plate due to thermal load is treated as an initial geometric imperfection having the same shape as the buckling mode. Such imperfection amplitude can be obtained as a function of the temperature. The postbuckling behavior is modeled using Koiter's theory of elastic stability. In the analysis, the plate at room temperature is assumed to be perfectly flat (zero imperfection amplitude) and, prior to the application of mechanical loads, the imperfection is assumed to be due to thermal loading only.

The thermal expansion coefficient of unidirectional graphite-epoxy plates in the fiber direction is known to be negative so that that the material expands upon cooling. Tsai and Hahn (1980) reported that a typical value for AS/3501 is -0.3×10^{-6} per °C. The values vary from zero to -3.0×10 per °C, and typical values were reported by Freeman and Campbell (1972), Lord and Dutta (1988) and Rondeau et al. (1988). The experimental value of the thermal expansion coefficient of the current set of graphite/epoxy composites determined by a Perkin-Elmer Thermo Mechanical Analysis System was -0.44×10^{-6} per °C (Dutta 1991).

The rectangular plates were simply supported at the

two loaded opposite edges and free in the remaining two unloaded edges. Such plates are known as wide beams. It should be noted that the buckling mode of a wide beam involves waviness both in the loading x-direction and in the in-plane y-direction (Fig. 1), whereas the buckling mode of an Euler column involves waviness only in the x-direction. Donnell (1976) found that the buckling load using the wide beam (plate) theory is only a few percent higher than that using the Euler buckling formula. In the present analysis, it is assumed that the postbuckling behavior of wide beam can also be predicted using the Euler column theory. Thus, in our analysis, the influence of waviness in the y-direction is neglected.

It is well known that the axial buckling load of a simply supported Euler column is

$$P_{cr} = \pi^2 EI/L^2 \tag{1}$$

where E is elastic modulus in the x-(fiber) direction, I, the moment of inertia ($= Bh^2/12$), L, the plate length, B, the width, and h, the plate thickness.

The postbuckling behavior of an Euler column was analyzed by Koiter (1945) and Hui and Hansen (1980), among others. Using the terminology employed by Budiansky and Hutchinson (1964) and Hui (1984), the postbuckling behavior is described by

$$(b)(\delta/h)^3 + (1 - [P/P_{cr}])\,(\delta/h) = (P/P_{cr})\,(\bar{\delta}/h) \tag{2}$$

where b is the postbuckling coefficient, $\bar{\delta}$ is the amplitude of the initial geometric imperfection, δ is the amplitude of the out-of-plane deflection (measured from the imperfect position) and P is the applied compressive load. From Hui and Hansen (1980), it can be shown that

$$b = (\pi^2/8)\,(h/L)^2 \tag{3}$$

which is essentially zero for $h << L$ in plates. Defining $\lambda = P/P_{cr}$, it follows that

$$\delta = \bar{\delta}\,\lambda/(1 - \lambda) \tag{4}$$

It should be noted that the postbuckling theory is based on an asymptotic analysis, which is valid only for a sufficiently small amplitude of the imperfection (say $\bar{\delta}/h < 1.5$).

The thermal strain ε_T in the x-direction of the plate is given by

$$\varepsilon_T = \Delta L/L = (\alpha)\,(\Delta T) \tag{5}$$

where α is the coefficient of thermal expansion in the fiber direction (negative means that the plate will expand upon cooling) and ΔT is the current temperature minus the reference temperature (room temperature). The thermal buckling problem occurs only when $(\alpha)\,(\Delta T)$ is positive with in-plane constraint.

If the deflection profile of the simply supported plate due to thermal loading alone is assumed to be of the sinusoidal shape,

$$w = \bar{\delta} \sin(\pi x/L) \tag{6}$$

where w is the out-of-plane deflection, x is measured from the loaded edge and $\bar{\delta}$ is the amplitude of the "imperfection" due to thermal loading. The arc length $L + \Delta L$ can be obtained from (Fig. 2):

$$L + \Delta L = \int_{x=0}^{L} \sqrt{\left[1 + \left(dw/dx\right)\right]^2}\, dx. \tag{7}$$

Substituting the deflection w into the arc length expression and integrating and solving for the imperfection amplitude $\bar{\delta}$, one obtains

$$\bar{\delta}/h = [2/(\pi h)]\,(L)\,(\Delta L/L)^{1/2} \tag{8}$$

where h is the thickness of the laminated plate. From the thermal strain (eq 5), the imperfection amplitude can

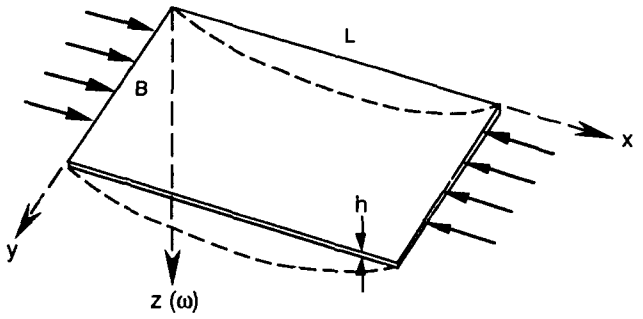

Figure 1. Reference coordinates of the buckling problem.

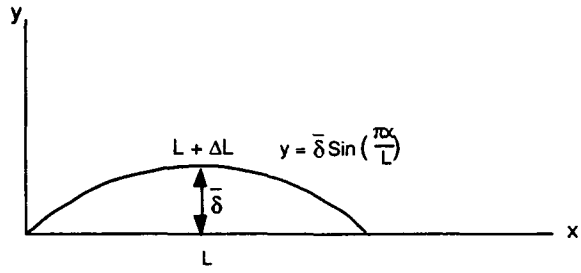

Figure 2. Deflection profile of the plate from thermal stress.

also be written as

$$\bar{\delta}/h = [2/(\pi h)]\,(L)[\alpha(\Delta T)]^{1/2}\,. \tag{9}$$

Solving for the load ratio λ and using eq 9, one obtains

$$\lambda = \frac{(\delta/h)}{(\delta/h) + [2L/(\pi h)]\,[\alpha(\Delta T)]^{1/2}}\,. \tag{10}$$

In order to detect bending of the plate, the strains are measured at the center of the plate on both surfaces (Fig. 3). The measured strains at *aa* and *bb* are, respectively,

$$\begin{aligned} \varepsilon_A &= (s_A/s_C) - 1 < 0 \qquad \text{compression} \\ \varepsilon_B &= (s_B/s_C) - 1 > 0 \qquad \text{tension} \end{aligned} \tag{11}$$

where s_A, s_B and s_C denote the arc length *aa*, *bb* and *cc*.

In the case of thermal loading only (no mechanical load), the measured strains are denoted by ε_A^o and ε_B^o. Since the tensile and compressive modulus are different, ε_A^o will not be the same as ε_B^o. Likewise, in general, ε_A is not the same as ε_B.

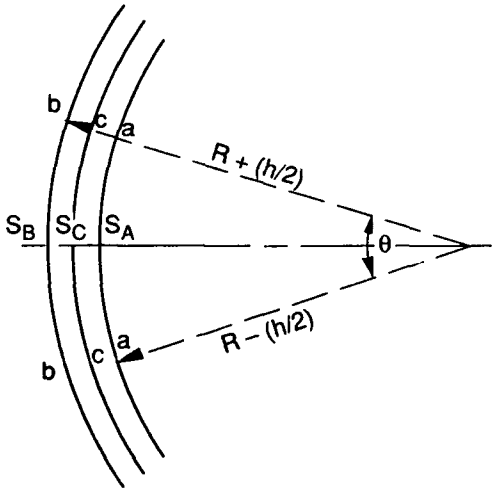

Figure 3. Bending of the plate.

From these strains, the deflection can be obtained using the curvature expression (Roark and Young 1975):

$$1/R = M/(EI) \tag{12}$$

Since, in bending of a beam $M = (EI)(d^2w/dx^2)$, it follows that

$$1/R = d^2w/dx^2 \tag{13}$$

where R is the radius of curvature of the beam and M is the bending moment. Note that both R and M are functions of x, and the product R, and M is a constant. If the deflection shape is assumed to be a half sine wave,

$$w = (\delta + \bar{\delta})\sin(\pi x/L)\,. \tag{14}$$

Substituting the deflection into eq 12 and 13, one obtains

$$\delta + \bar{\delta} = L^2/(R\pi^2)\,. \tag{15}$$

From Figure 3, the angle θ is defined to be

$$\theta = \frac{s_A}{R - (h/2)} = \frac{s_B}{R + (h/2)} \tag{16}$$

so that

$$R = (h/2)\,[(s_A/s_C) + (s_B/s_C)]\,/\,[(s_B/s_C) - (s_A/s_C)] \tag{17}$$

Substituting s_A/s_C and s_B/s_C from eq 11 into eq 15 and 17, one obtains

$$(\delta + \bar{\delta})/h = \frac{2\,[L/(h\pi)]^2\,(\varepsilon_B - \varepsilon_A)}{2 + \varepsilon_A + \varepsilon_B}\,. \tag{18}$$

Since $\varepsilon_A + \varepsilon_B << 2$, no significant error will occur from their omission in the denominator. The deflection δ/h can then be obtained from the offsetted strains $\varepsilon_B - \varepsilon_B^o$ and $\varepsilon_A - \varepsilon_A^o$ such that

$$\delta/h = [L/(h\pi)]^2\,[(\varepsilon_B - \varepsilon_B^o) - (\varepsilon_A - \varepsilon_A^o)] \tag{19}$$

where ε_A^o and ε_B^o are the strains due to thermal loading only.

EXPERIMENTAL METHOD

The experimental buckling behavior of the unidirectional graphite fiber/epoxy plates was examined using

Table 1. Material specifications of the test composite panels.

Manufacturer	Fiberite Corporation
Fiber type	T-300 graphite
Resin	Fiberite 974 epoxy
No. of plys/lay up	Eight/unidirectional
Thickness/ply	0.136 mm (0.00537 in.)
Total thickness	0.965 mm (0.038 in.)
Density	1522.4 kg/m^3 (0.055 lb/in.^{3})
Fiber vol %	55
Major Poisson's ratio	0.25
Longitudinal compr. modulus	147.6 GPa (21.4×10^6 lbf/in.^{2})
Longitudinal tension modulus	169.7 GPa (24.6×10^6 lbf/in.^{2})
Transverse tension modulus	10.14 GPa (1.47×10^6 lbf/in.^{2})
Shear modulus	4.62 GPa (0.67×10^6 lbf/in.^{2})
Longitudinal tensile strength	2.621 GPa (380×10^3 lbf/in.^{2})
Longitudinal compr. strength	1.034 GPa (150×10^3 lbf/in.^{2})
Transverse tensile strength	60.0 MPa (8.7×10^3 lbf/in.^{2})

a servohydraulic testing machine to apply a quasi-static load in the fiber direction (0°). The frame of the machine is enclosed in an environmental chamber connected to a refrigeration unit to test at low temperatures. The plates were supported at the edges using bearing-mounted components to allow for free rotation at the edges. At the center of each plate, rosette strain gauges were mounted "back-to-back" on either side. The outputs of the six strain gauges were passed through a Wheatstone bridge, while the applied load and displacement were monitored and recorded using a datalogger system and then sent directly to a personal computer.

The composite plates tested in the experiment were manufactured by Fiberite Corporation as eight-ply unidirectional T-300 graphite fibers in a 974 epoxy resin matrix. The material specifications are listed in Table 1.

The plates were carefully cut to avoid heating the edges to 127 × 254 mm (5 × 10 in.) using a diamond blade on a band saw. The plates were then examined with a dial gauge to determine the flatness and initial

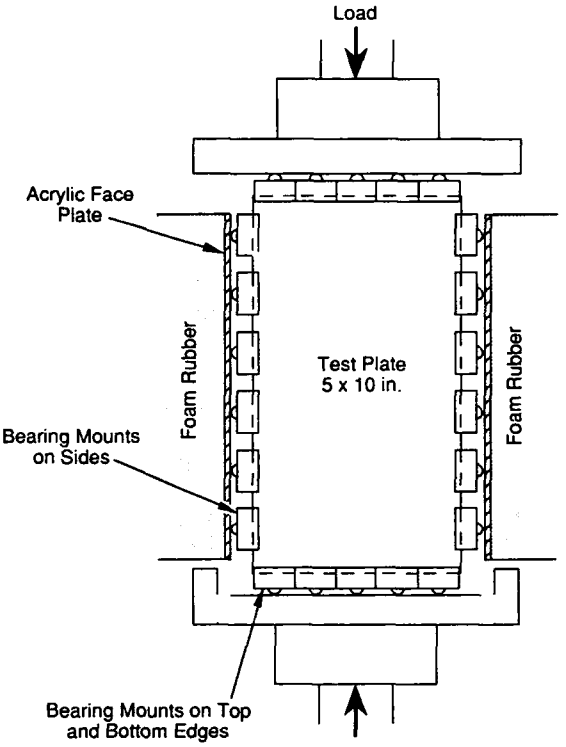

Figure 4. Test configuration for buckling of plates.

imperfections of each sample. These readings indicated that the plates were flat with variations in the thickness of up to 0.125 mm (0.005 in.). Rosette strain gauges were then mounted on the surface of each plate on both sides in a back-to-back configuration.

The experimental setup is illustrated in Figure 4. The system consisted of the plate mounted on the bearings which were supported by specially designed fixtures on the top and the bottom, and, for negligible support, by foam-backed plexiglass plates on the sides that were made to fit against the sides of the environmental chamber.

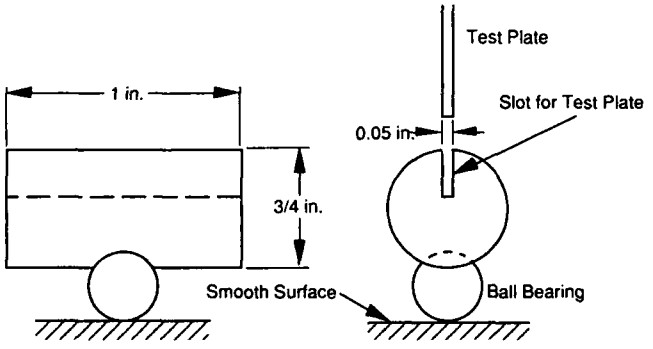

Figure 5. Bearing-mounted simple support.

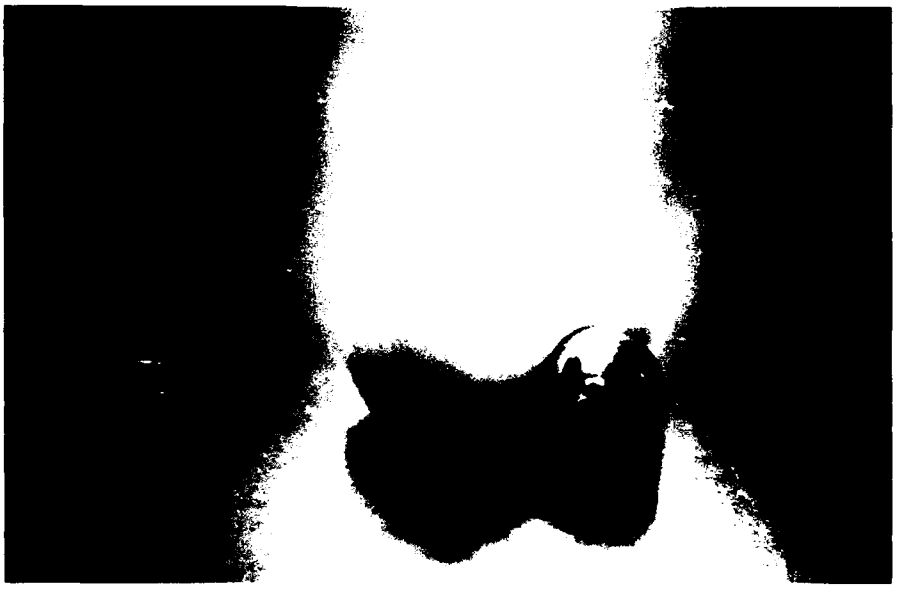

Figure 6. Photograph of the bearing-mounted simple support.

The design of the bearing mounted supports is shown in Figures 5 and 6. A 19-mm (3/4-in.) Teflon rod machined to create a 1.3-mm (0.05-in.) slot and a 1.6-mm- (0.063-in.-) diam. hole along the entire length and then cut into 25.4-mm (1-in.) cylinders was used as the body of the support. A semicircular identation was made to a depth of 3.2 mm (0.125 in.) to accommodate the 12.7-mm (0.5-in.) stainless steel ball bearing. The bearings were attached to the Teflon using a thin coat of adhesive.

The loading frames on the top and bottom were made from 19-mm (3/4-in.) aluminum plates with a 25.4-mm (1-in.) diameter hole in the center tapped to 14 turns per inch to fit onto the testing machine thread. The plates served as a flat loading surface through the ball bearings during the test. The load was applied at the rate of 0.625-mm (0.025-in.) per minute cross head speed.

The servohydraulic testing machine with its environmental chamber attached to a refrigeration unit is shown in Figure 7. Insulation was placed at the openings around the upper and lower pistons of the testing ma-

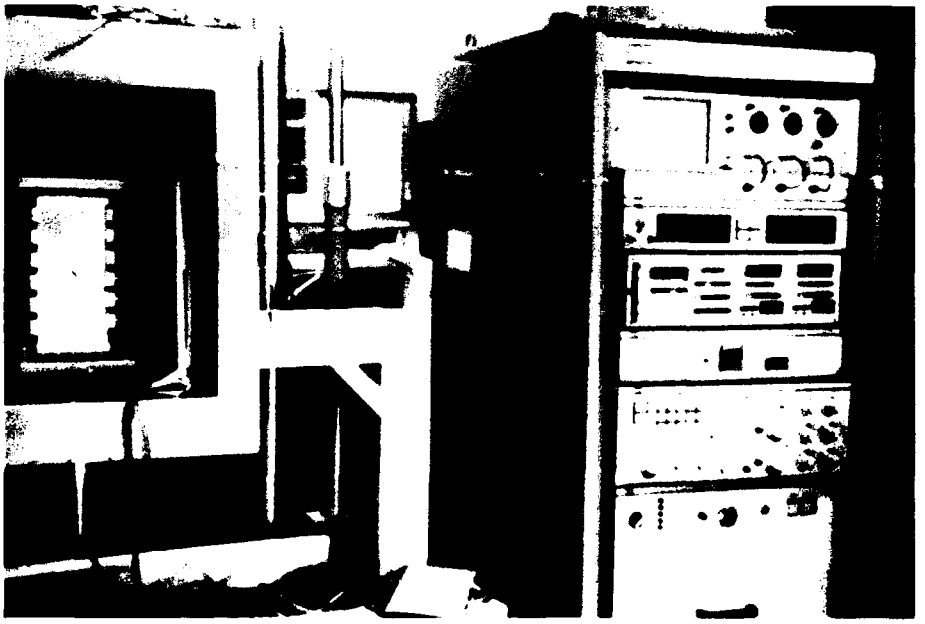

Figure 7. MTS servohydraulic test machine with environment chamber.

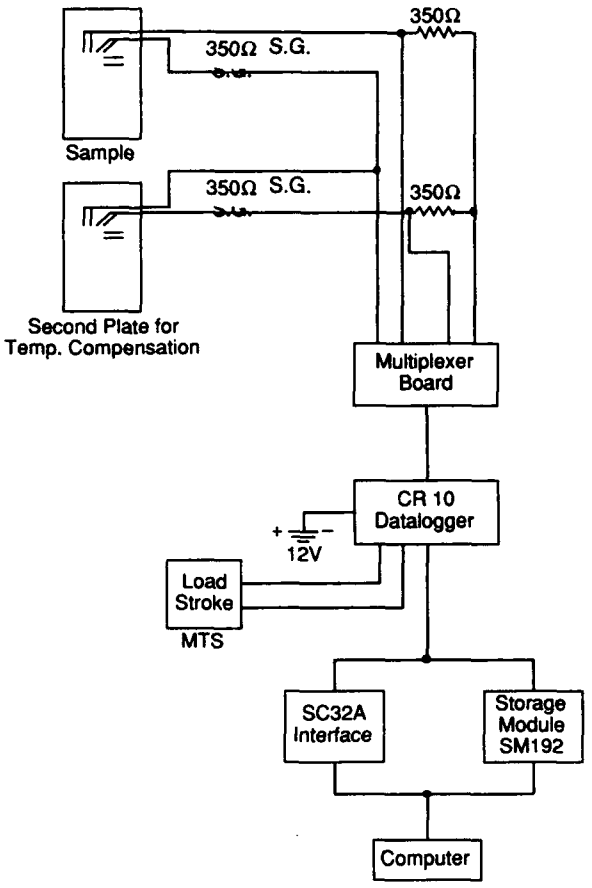

Figure 8. Schematic of test and data collection system.

chine and also at a side port for the strain gauge wires. This allowed for the strain gauge instrumentation and the load cell to be protected at ambient temperature.

The test procedure required that the specimen be perfectly aligned. This was achieved by first attempting to visually set up the specimen supports along the guidelines of the fixtures, adjusting the strain gauge electrical instrumentation, applying a small pre-load, and then carefully adjusting the specimen by the strain gauge output monitored by the computer.

After alignment of the specimen, the load was applied until the specimen displayed a significant out-of-plane displacement. The load was then removed from the plate and the data were downloaded to a computer for analysis. A schematic of the instrumentation and data collection system is shown in Figure 8.

EXPERIMENTAL RESULTS

The experimental results indicate some interesting behavior in the buckling and postbuckling modes for the composite plates. The effect of lower temperature on this behavior is apparent upon comparison of the results to those from tests done at ambient temperature.

Table 2 gives the summary of the results. The data from a typical test are shown in Figure 9 in which the applied stress and resultant axial strains are plotted with respect to time. It can be seen that the stress increases proportionally with the strain until the point of bifurca-

Table 2. Experimental buckling results.

Test	*Plate*	*Temperature (°C)*	*Maximum stress MPa (lbf/in.²)*	*Buckling stress MPa (lbf/in.²)*
C2AR	C2	21.0	1.692 (245.38)	1.645 (238.54)
R4DR	R4	21.0	1.664 (241.33)	1.418 (205.64)
C4AR	C4	21.0	1.343 (194.67)	0.529 (76.77)
C3AR	C3	21.0	2.231 (323.55)	1.730 (250.92)
R3AC	R3	-6.1	1.210 (175.52)	0.416 (60.3)
C5BC	C5	-9.6	1.314 (190.56)	1.229 (178.26)
C5DC	C5	-11.2	1.116 (161.75)	0.492 (71.28)
R4BC	R4	-11.3	1.645 (238.58)	1.277 (185.10)
R4AC	R4	-13.3	1.626 (235.79)	1.182 (171.37)
R2CC	R2	-14.0	1.370 (198.77)	0.567 (82.25)
R3BC	R3	-16.0	1.475 (213.91)	0.484 (78.17)
R3CC	R3	-17.8	1.503 (218.02)	0.482 (69.92)
R2BC	R2	-19.0	1.324 (191.98)	0.511 (74.03)
R2AC	R2	-19.0	1.333 (193.33)	0.492 (71.33)

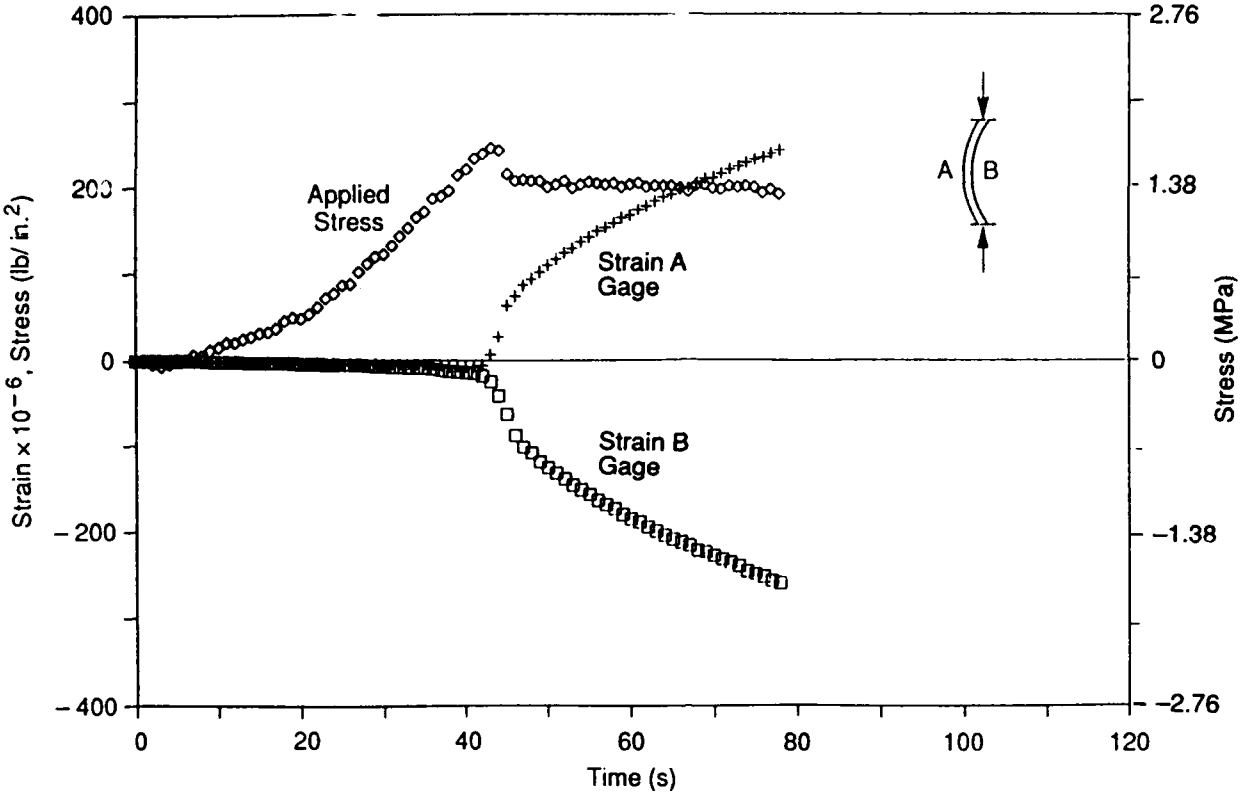

Figure 9. Stress and strain history of buckling load.

tion of the outputs from the two back-to-back strain gauges, A and B, on opposite surfaces at the center of the plate. This point of bifurcation indicates that the specimen has buckled, and the out-of-plane displacement occurred such that one side of the plate had gone in compression as the other side went in tension. However, the plate continues to support additional loading in the post-buckling range as the strain continues to increase. The highest load sustained and the buckling load found from the point of bifurcation of the axial strain gauges are listed in Table 2.

The axial strain at four different temperatures given by gauges A and B vs stress is shown graphically in Figure 10. A review of these graphs demonstrates a marked difference in the buckling and postbuckling paths as the temperature is decreased. Figure 10a shows that, following a linear elastic deformation, at room temperature the plate buckles at a well-defined critical load P_{cr} (approximately 1.2 MPa (175 lbf/in.^{2}). But at lower temperatures the sharp, well-defined buckling load is absent: the curves of buckling path are progressively flatter from −10° to −19°C as shown in Figures 10b through 10d. A series of smooth curves drawn through the data points of each of the above figures are superimposed and shown in Figure 10e. It is clear from Figure 10e that lower temperature represents a higher degree of initial geometric imperfection, as discussed before.

The stress vs axial strain is plotted for small loads (before buckling) in Figure 11, for a representative plate using a regression analysis to confirm that the modulus of elasticity is consistent with the specifications provided by the manufacturer. These graphs serve only as an indicator, as these plates do not have a suitable geometry to determine the compressive moduli. However, it does show the characteristic stress-strain behavior, which was within the range of specifications of the laminate plate.

In Table 2 the data are arranged in order of ambient to decreasing temperatures to see the effect on the load capacity. Four basic ranges of temperature, 21°, −10°, −15°, and −20°C, are grouped. The buckling stresses were determined by an estimate of the stress at the point of departure from linearity. The maximum stress is usually the stress at which the test was terminated.

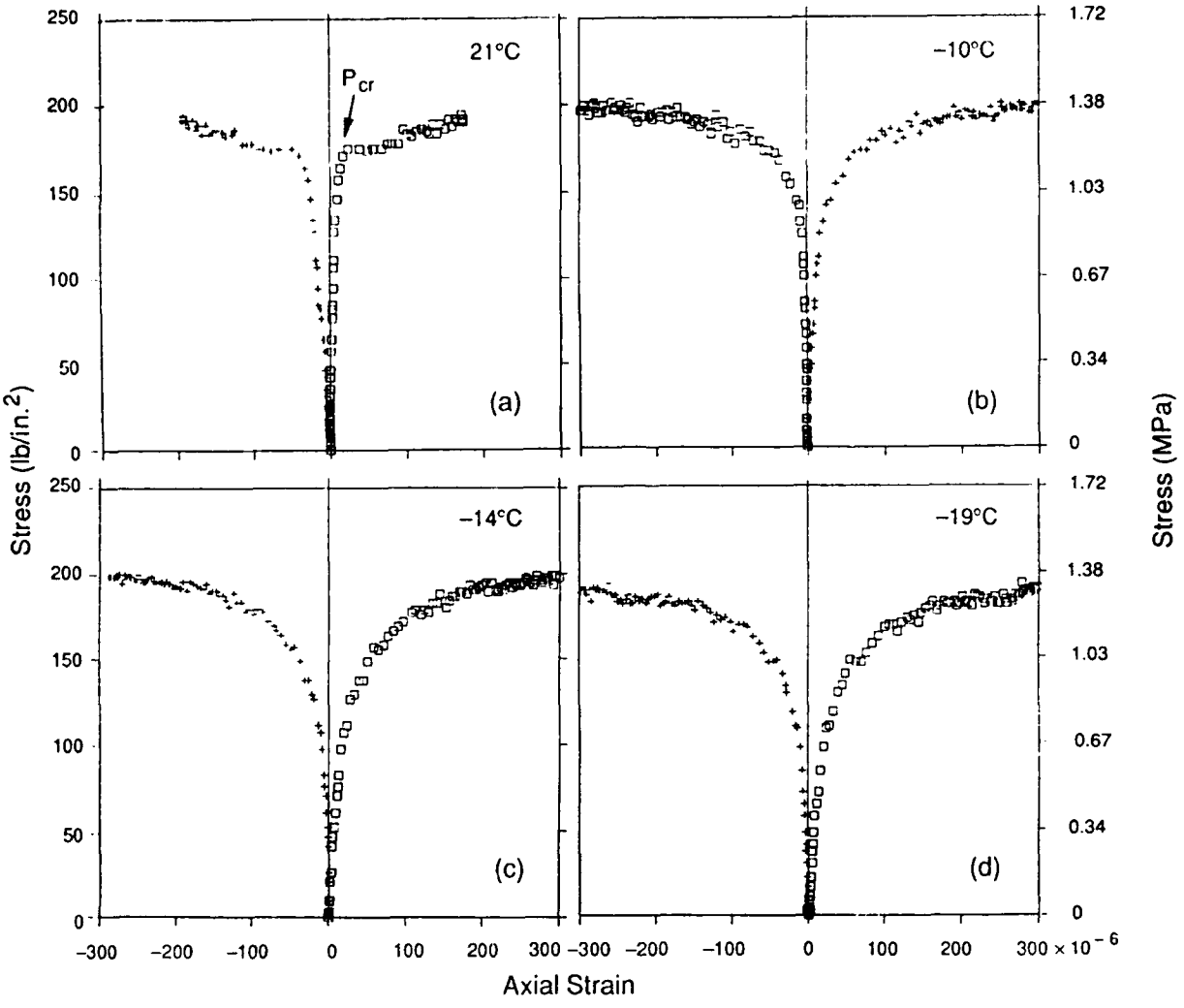

a–d. Paths at 21°, –10°, –14° and –19° C.

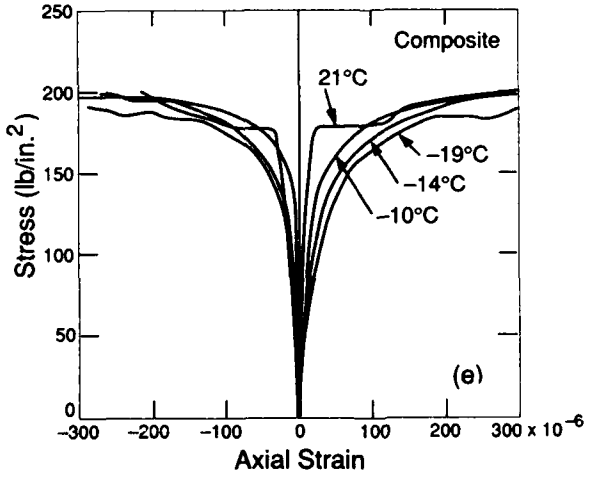

e. Composite of the paths showing effect of temperature.

Figure 10. Buckling and postbuckling paths at different temperatures.

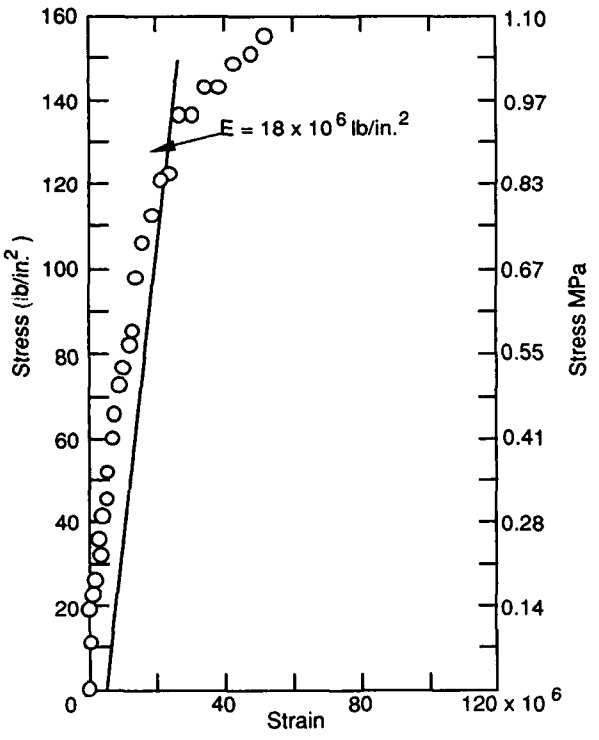

Figure 11. Axial stress-strain data of a typical panel before buckling.

DISCUSSION OF RESULTS

The focus of this study is to determine experimentally the effect of low temperature on the buckling behavior of graphite fiber-epoxy composite. The unidirectional simply-supported plate was chosen, so that this effect could be isolated from other interlaminar stresses for examination. The results show interesting characteristics that are discussed here.

In testing the specimen the bearing mounts described above sucessfully provided simple support on the top and bottom and the boundary conditions on the sides provided free edges. The plates did buckle, having simple support in the axial direction as an Euler column, as described in the theory section.

The results show very significant changes in the buckling and postbuckling behavior at ambient and low temperatures as illustrated by a model shown in Figure 12. The point of bifurcation and load carrying capacity appear significantly reduced as the temperature is decreased. The postbuckling path also dramatically changed at low temperatures, giving the apperance of less brittle behavior. In developing the theory, we discussed that this behavior could be expected due to higher imperfection amplitudes induced as the temperature is decreased.

Figure 13 shows the postbuckling curves of the applied load ratio λ (i.e., P/P_{cr}) vs the deflection ratio (δ/h) as a function of the imperfection amplitude ratio ($\bar{\delta}/h$). It can be seen that room temperature corresponds to zero imperfection amplitude and the plate will remain flat for $P < P_{cr}$. For a given imperfection amplitude (due to thermal load), the out-of-plane deflection occurs even at no mechanical load. The application of mechanical load will further increase the deflection. As the imperfection amplitude increases, the above trends become more pronounced. Therefore, with reduction of temperature, imperfection amplitudes will increase, resulting in the characteristic buckling and postbuckling path shown in Figure 12.

Figure 14 shows the buckling and postbuckling paths of three plates tested at −19, −14, and −9.6°C. These results were obtained from the experimental load ratio

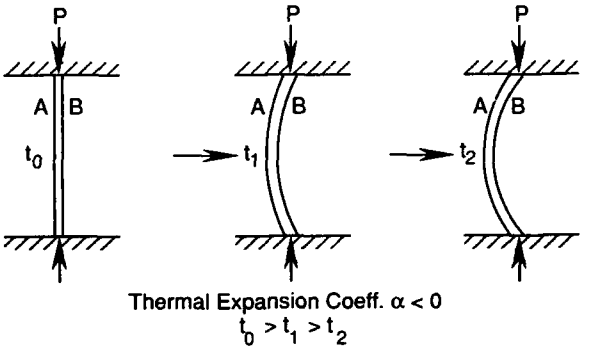

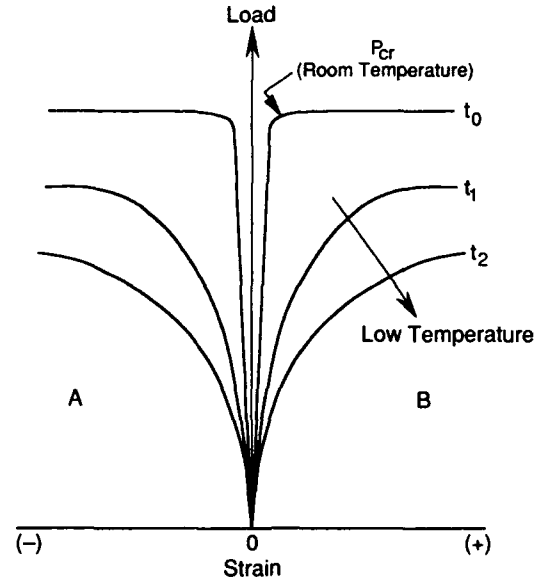

Figure 12. Influence of low temperature on 0° graphite/epoxy composite buckling.

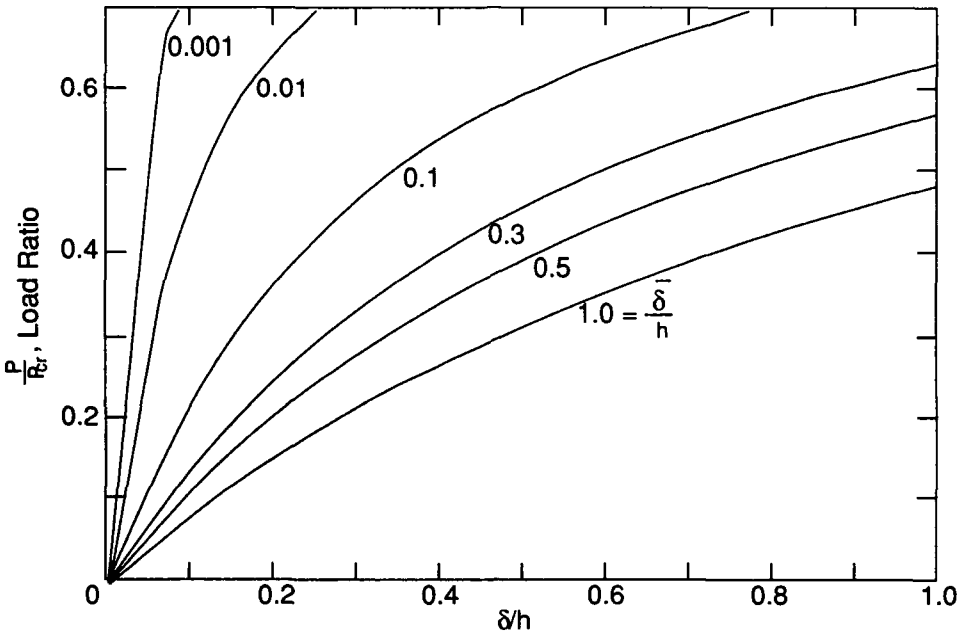

Figure 13. Predicted behavior of unidirectional plates under buckling load with initial imperfection developed from thermal strain.

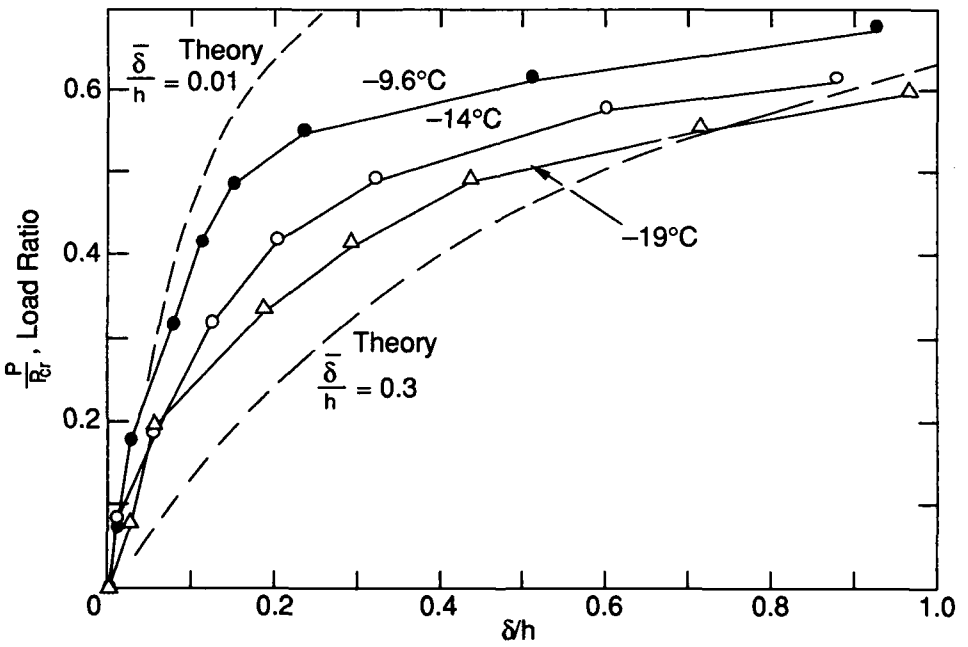

Figure 14. Comparison of experimental buckling data with theory.

and the corresponding strain data. These paths lie between the paths corresponding to imperfection amplitude ratio ($\bar{\delta}/h$) = 0.01 and 0.3 plotted by using eq 19. If Mallick's (1988) data for T-300 fiber thermal expansion coefficient of -0.1×10^{-6} m/m per °C are used, the initial geometric imperfection ($\bar{\delta}/h$) from eq 9 varies from 0.29 at −10°C to 0.33 at −20°C. Thus, it can be seen that the theory slightly overestimates the buckling, but the trend of the buckling curves clearly agrees with that predicted by the postbuckling theory. The theory established that with lower temperature the imperfection amplitude is higher.

CONCLUSION

The current work on the unidirectional graphite/epoxy laminate is particularly interesting since such plates, because of their negative thermal expansion coefficient, expand in the fiber direction on cooling, but bend when constrained without any mechanical load. A theoretical treatment of the problem has been developed to show that the out-of-plane bending could be treated as an initial geometric imperfection. The postbuckling theory based on this initial imperfection model was validated by a series of experimenal data obtained from testing the laminates at various low temperatures. The experimental postbuckling curves under combined thermal and mechanical loads show the effect of increasing severity of initial geometric imperfection with decreasing temperatures.

The implication of a plate's bending due to negative thermal expansion coefficient is very significant in design considerations. Obviously, when the ambient temperature drops, such constrained plates are actually buckled already (the structure is weakened significantly) even before the application of the mechanical compressive load. The induced bending effect at low temperatures turns out to dominate the stiffening effect in the buckling experiments. Thus, in the design of plates against buckling in cold regions, it is important to take into account the in-plane constraint causing the premature bending of the plate due to thermal cooling alone.

LITERATURE CITED

Biswas, P. (1976) Thermal buckling of orthotropic plates. *ASME Journal of Applied Mechanics*, June, p. 361–363.

Budiansky, B. and J.W. Hutchinson (1964) Dynamic buckling of imperfection sensitive structures. In *Proceedings of 11th International Congress of Applied Mechanics, Munich* (H. Gortler, Ed.), New York: Springer-Verlag, p. 636–651.

Chen, L.W. and L.Y. Chen (1987) Thermal buckling of laminated composite plates. *Journal of Thermal Stresses*, **10:** 345–356.

Chen, J.K., C.T. Sun and C.I. Chang (1985) Failure analysis of a graphite/epoxy laminate subjected to a combined thermal and mechanical loading. *Journal of Composite Materials*, **19:** 408–441.

Dutta, P.K. (1991) Thermal expansion coefficient of fiberite graphite/epoxy composites. CRREL Technical Note (unpublished).

Donnell, L.H. (1976) *Beams, Plates and Shells.* New York: McGraw Hill, p. 199.

Flaggs, D.L. and J.R. Vinson (1978) Hygrothermal effects on the buckling of laminated composite plates. *Fiber Science and Technology*, **11**(5): 353–365.

Freeman, W.T. and M.D. Campbell (1972) Thermal expansion characteristics of graphite reinforced composite materials. In *Composite Materials: Testing and Design (Second conference)* (H. T. Corten, Ed.), ASTM-STP-497, American Soc. of Testing and Materials, p. 121–142.

Hui, D. (1984) Effects of mode interaction on collapse of short, imperfect thin walled columns. *ASME Journal of Applied Mechanics*, **51**(3): 566–573.

Hui, D. and J.S. Hansen (1980) The swallowtail and butterfly cuspoids and their application in the initial post buckling of single mode structural systems. *Quarterly of Applied Mechanics*, April, p. 17–35.

Jones, R.M. (1975) *Mechanics of Composite Materials.* New York: McGraw Hill, p. 239–285.

Koiter, W.T. (1945) On the stability of elastic equilibrium. Doctoral Thesis, Delft, The Netherlands (NASA-Tech Trans F10,833,1967 and AFFDL-TR-70-25, (1970).

Leissa, A.W. (1985) Buckling of laminated composite plates and shell panels. Air Force Wright Aeronautical Laboratory Report AFWAL-TR-85-3069.

Lord, H.W. and P.K. Dutta (1988) On the design of polymeric composite structures for cold regions applications. *Journal of Reinforced Plastics and Composites*, **7:** 435–458.

Roark, R.J. and W.C. Young (1975) *Formulas for Stress and Strain.* New York: McGraw Hill, p. 91.

Rondeau, R.A., D.R. Askins and P. Sjoblom (1988) Development of engineering data on aerospace materials. Air Force Wright Aeronautical Laboratory Report AFWAL-TR-88-4217, December, p. 412.

Singer, J. (1985) Experimental techniques and comparison. In *Buckling and Postbuckling* (E. Araki, Ed.). New York: Springer-Verlag.

Tsai, S.W. and H.T. Hahn (1980) *Introduction to Composite Materials*, Lancaster, Pennsylvania: Technomic Publishing Co., p. 344.

REPORT DOCUMENTATION PAGE

Form Approved
OMB No. 0704-0188

1. AGENCY USE ONLY (Leave blank)	2. REPORT DATE	3. REPORT TYPE AND DATES COVERED
	November 1991	

4. TITLE AND SUBTITLE
Buckling of Unidirectional Graphite/Epoxy Composite Plates at Low Temperatures

5. FUNDING NUMBERS
PR: 4A762784AT42
TA: SS
WU: 019

6. AUTHORS
Piyush K. Dutta, David Hui, and Yvonne M. Traynham

7. PERFORMING ORGANIZATION NAME(S) AND ADDRESS(ES)
U.S. Army Cold Regions Research and Engineering Laboratory
72 Lyme Road
Hanover, N.H. 03755-1290

8. PERFORMING ORGANIZATION REPORT NUMBER
Special Report 91-20

9. SPONSORING/MONITORING AGENCY NAME(S) AND ADDRESS(ES)
Office of the Chief of Engineers
Washington, D.C. 20314-1000

10. SPONSORING/MONITORING AGENCY REPORT NUMBER

11. SUPPLEMENTARY NOTES

12a. DISTRIBUTION/AVAILABILITY STATEMENT
Approved for public release; distribution is unlimited.

Available from NTIS, Springfield, Virginia 22161.

12b. DISTRIBUTION CODE

13. ABSTRACT (*Maximum 200 words*)

A theoretical and experimental study of the buckling and postbuckling behavior of unidirectionally laminated graphite/epoxy plates was conducted under combined thermal cooling and compressive loading. The rectangular plates were simply supported at the loaded edges and free in the remaining edges. The plates were found to bend during cooling even without mechanical loads because of the negative thermal expansion coefficient of the material in the loading direction and the in-plane end constraints at the two loaded edges. Such bending from thermal load was treated as an initial geometric imperfection, and the analysis was based on Koiter's theory of elastic stability. The experimental postbuckling curves agreed well with the theoretical values.

14. SUBJECT TERMS
Bending, Buckling, Cold regions, Composites, Fiber composites, Graphite/epoxy composites

15. NUMBER OF PAGES
17

16. PRICE CODE

17. SECURITY CLASSIFICATION OF REPORT	18. SECURITY CLASSIFICATION OF THIS PAGE	19. SECURITY CLASSIFICATION OF ABSTRACT	20. LIMITATION OF ABSTRACT
UNCLASSIFIED	UNCLASSIFIED	UNCLASSIFIED	UL

NSN 7540-01-280-5500

☆ U. S. GOVERNMENT PRINTING OFFICE: 1992--600-063--42042

Standard Form 298 (Rev. 2-89)
Prescribed by ANSI Std. Z39-18
298-102